iJRASET
International Journal For Research in Applied Science and Engineering Technology

INTERNATIONAL JOURNAL FOR RESEARCH

IN APPLIED SCIENCE & ENGINEERING TECHNOLOGY

Volume: 12 **Issue:** I **Month of publication:** January 2024

DOI: https://doi.org/10.22214/ijraset.2024.58032

www.ijraset.com

Call: 08813907089 | E-mail ID: ijraset@gmail.com

International Journal for Research in Applied Science & Engineering Technology (IJRASET)
ISSN: 2321-9653; IC Value: 45.98; SJ Impact Factor: 7.538
Volume 12 Issue I Jan 2024- Available at www.ijraset.com

Copper Nano Particles Decorated CNMs from Plant Fiber as Superconducting Material

B.T. Mukherjee[1], Shyambabu K. Sainik[2]
Department of Chemistry, K. V. Pendharkar College of Arts, Science and Commerce (Autonomous), Dombivli, 421203, India.

Abstract: ***The negative dielectric constant has been attracting attention of many researchers due to its significant applications viz. superconductor, in this present work, carbon nano materials (CNM) have been synthesized from plant fiber (cotton) for the negative dielectric constant 'meta-materials' study. The synthesized CNM was decorated with copper nano particles confirmed with the XRD. Whereas obtained material is a mixture of amorphous and graphitic carbon, confirmed by Raman spectroscopy. SEM and TEM images of the carbon filaments indicates that the CNF have 30 to 50 nm thicknesses with 357.3 nm diameters while decorated copper nano particles are in between 50-70 nm range in size respectively. The obtained materials show very poor microwave absorption, however the negative dielectric constant value observed is -1000000×8.85×10^{12}in the frequency range of 1.54 ×10^{9} Hz to 1.35×10^{10} Hz. This outstanding material nominates itself as an excellent superconducting material.***

Keywords: Carbon Nano Materials, Meta-materials, Microwave absorption, Negative dielectric constant, Superconducting material.

I. INTRODUCTION

Many researchers have focused their efforts on materials exhibiting positive dielectric constants or permittivity [1-3]. Materials with positive dielectric constants are poor conductors of electricity, functioning as insulators that impede the flow of current. These materials find applications in various electronic devices, with those featuring low dielectric loss utilized for novel capacitance to achieve high-density energy storage. Additionally, high dielectric constant materials are employed in semiconductors to enhance performance and reduce device size [4-5].

In contrast, negative dielectric constant materials, often referred to as 'meta-materials', have garnered significant attention due to their exotic properties.

These materials have diverse applications, including the production of high-temperature superconductors, use in optical devices, electrically tunable microwave devices, and the creation of negative refractive index materials [6-17]. Despite the promising potential of negative dielectric constant materials, there is limited literature available on this subject.

The negative dielectric permittivity of polyvinyl difluoride nano-composites induced by carbon nano-fibers (CNF) was studied. It revealed that the negative permittivity increases with the growing amount of CNF, achieving a remarkable -2500 negative dielectric permittivity with 5% CNF at 5 kHz [18].

Similarly, the investigation of negative dielectric permittivity using antimony tin oxide ceramics revealed similarities in dielectric loss to that observed in plasma [19].The negative dielectric constant properties of barium titanate/Nickel meta-composites confirmed that 35.56% Nickel content was necessary to achieve negative permittivity and permeability in BaTiO3/Ni composites [20].

The exploration of the negative permittivity and electromagnetic shielding performance of silver/silicon nitride meta-composites suggested a shift in composite conductivity characteristics from hopping conductivity to metal-like conductivity as the percentage of silver increased [21].

Similar studies on La0.8Co0.2-xEuxTiO3 nano-rods, exhibited a maximum negative dielectric constant of -78.68 and a dielectric loss of -202.84.

Currently, a limited number of researchers are exploring negative dielectric constants using carbon nanomaterials (CNM) derived from renewable sources such as plant fibers. These CNMs boast excellent electrical, mechanical, thermal, optical, chemical, and catalytical properties, combined with their lightweight and high surface area [22-27].

In the current study, CNMs are synthesized using plant fibers, specifically cotton, adding to the growing body of research in the field of negative dielectric constants.

II. EXPERIMENTAL

The utilized materials comprised plant fibers, specifically commercial cotton. All the chemicals used were sourced from SDFCL and employed without undergoing additional purification processes.

A. Synthesis of Carbon Nano Materials (CNM's)

To prepare CNMs, cotton fibers underwent treatment with KOH followed by loading of copper and pyrolysed at 650°C in the presence of an inert gas using a Horizontal furnace. Mukherjee *et. al.* has provided a comprehensive explanation of the pyrolysis method for synthesizing CNMs from plant-based precursors [29-31].

B. Characterization

The sample underwent characterization through various techniques, including Scanning Electron Microscopy (SEM), Transmission Electron Microscopy (TEM), X-Ray Diffraction (XRD), and Raman Spectroscopy. Surface morphology of the CNMs was examined using a Hitachi S-4300 instrument for SEM imaging. The compositional and crystallographic structure of CNMs was studied through TEM imaging, recorded with a JEOL JEM-1011 microscope at an accelerating voltage of 100 kV. The XRD pattern, elucidating the crystallographic structure, was obtained using an X'Pert Philips instrument with a range of 2θ: 2.0000 <-> 80.0000°, employing Cu-Kα radiation (λ=1.54056 Å).Raman spectroscopy was employed to investigate the structure and crystalline phases of the sample, conducted using a Jobin Y'von Labram spectrometer with a laser excitation wavelength of 633 nm and a spectral resolution of <1.5 /cm. Microwave absorption (MA) studies for all prepared samples were performed using an N5249A PNA-X Vector Network Analyzer (VNA) over the frequency range of 9 kHz to 8.5 GHz. Dielectric constant was measured at ambient temperature to study dielectric property using an 85070-dielectric probe software (version E07.01.08) on an Agilent Technology N5221A MY514110A09.90.17 apparatus.

III. RESULT AND DISCUSSION

A. SEM

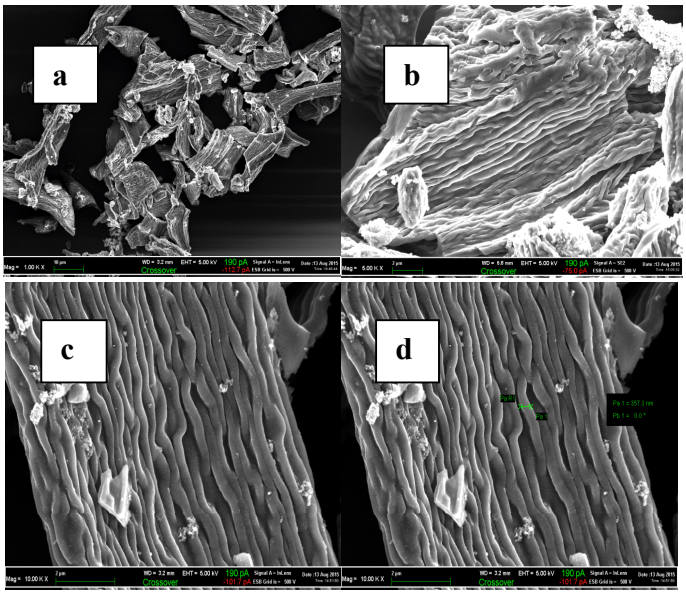

Fig. 1SEM images of CNM samples a-d

The SEM characterization is illustrated in Fig. 1. The images (a) and (b) revealed that the prepared sample takes the form of flakes. Image (c) provides a distinct view of the synthesized materials, displaying an original crest-like peculiar design and a fiber-like structure on the carbon surface. This observation is attributed to the material's preparation from plant fiber, evident in the image where numerous fibers are visibly interconnected. Additionally, Image (d) depicts carbon filaments with a diameter of 357.3 nm, and their thicknesses fall within the range of 30 to 50 nm.

B. TEM

Figure 2 presents the TEM image of the prepared CNMs sample, revealing the in-situ generation of metal nano-catalysts uniformly dispersed across the entire carbon surface. Additionally, the image illustrates that the metal particles are embedded on the carbon surface, exhibiting sizes within the range of 50-70 nm.

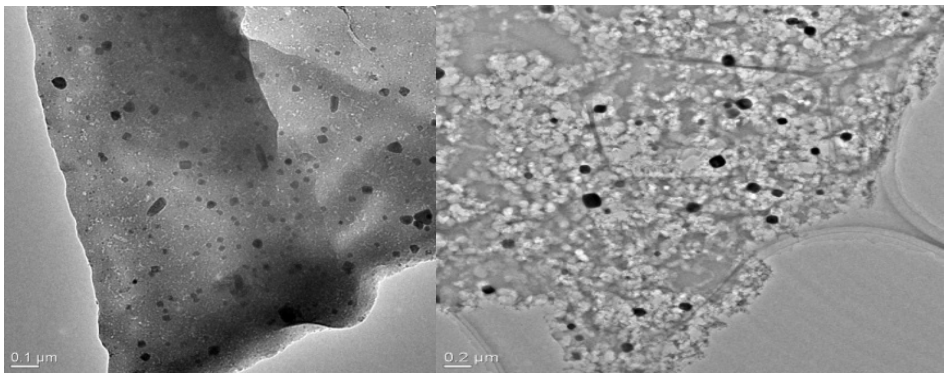

Fig. 2TEM images of CNM sample

C. Raman Spectrograph

The Raman spectrograph in Figure 3 exhibits two prominent peaks at 1349 cm^{-1} and 1504 cm^{-1}. The G band at 1479 cm^{-1} corresponds to the in-plane vibrational mode involving sp^2 hybridized carbon atoms in the graphene sheet, while the D band at 1231 cm^{-1} signifies the presence of structurally defected or disordered out-of-plane vibrational modes involving sp^3 carbon atoms. Notably, the D band exhibits a higher intensity than the G band, indicating the breakdown of sp^2 hybridized carbon atoms and their transformation into sp^3 hybridized carbon atoms. The ratio of the D/G band intensities suggests a higher prevalence of defective carbon compared to sp^2 hybridized carbon atoms.

Furthermore, a broad peak observed at 2648 cm^{-1} in all samples, varying in intensity, signifies the presence of amorphous carbon in the samples [32-33].

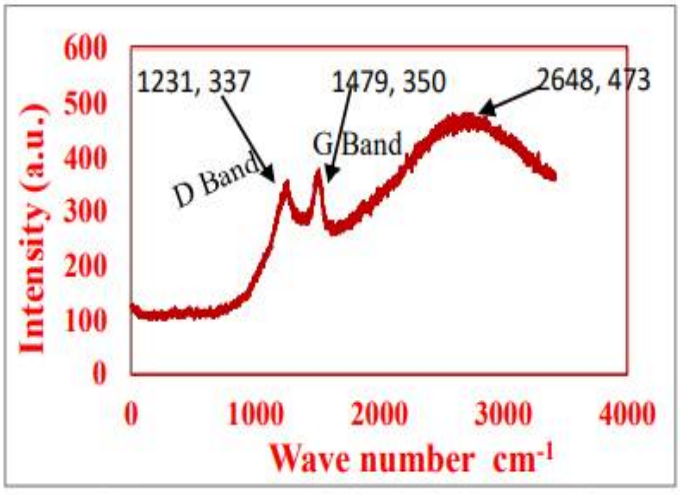

Fig.3.Raman spectrograph of synthesized CNM sample

D. X-Ray diffraction (XRD)

X-ray Diffraction (XRD) stands as a crucial and valuable tool for nanomaterials characterization. Figure 4 displays the XRD graph for the prepared CNMs sample. The CNMs graph data was collected for 2θ ranging from 10 to 80 degrees with a step size of 0.02 degrees. The initial peak observed near $2\theta = 11.40^{o}$ corresponds to Graphene Oxide (GO), while the broad peak at $2\theta = 23.20^{o}$ signifies the presence of Reduced Graphene Oxide (RGO) [34].

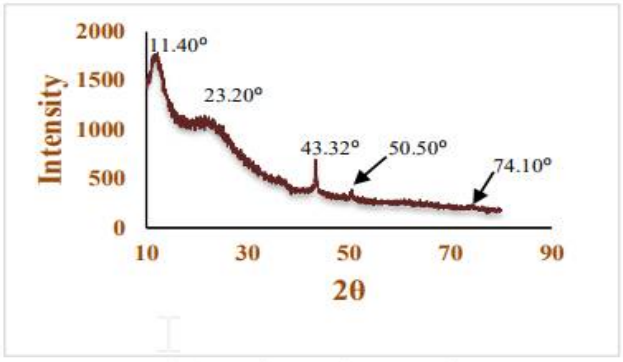

Fig.4.SEM images of CNM sample

Three additional peaks were observed at 2θ values of 43.32º, 50.50º, and 74.10º. These obtained values were compared with the standard powder diffraction card of JCPDS, copper file No. 04-0836, as detailed in Table 1. The analysis indicates that the prepared CNMs sample exhibits the presence of adorned copper nanoparticles with (1, 1, 1), (2, 0, 0), and (2, 2, 0) planes, respectively [35].

Experimental obtained CNM diffraction angle [2θ in degree]	Standard powder diffraction card of JCPDS, copper file No. 04-0836
43.32	43.297
50.341	50.433
74.108	74.130

Table 1.Comparison study of obtained CNM diffraction angle and Standard powder diffraction card of JCPDS

E. Microwave absorption

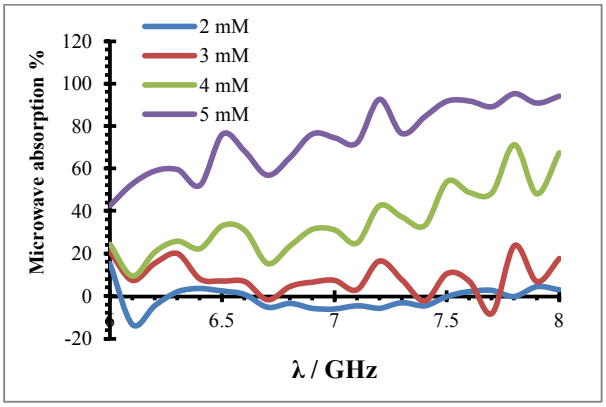

Fig.5.Microwave absorption study graph of synthesized CNM sample form 2-8 GHz frequency range.

The MA study of the synthesized materials was conducted using a VNA in the 2-8 GHz frequency range, corresponding to the S and C bands, with varying thickness from 2 to 5 mm as depicted in Figure 5. The S and C bands are utilized in applications such as surface ship radar, weather radar, Bluetooth, wireless LAN, long-distance radio telecommunication, RADAR, and satellite communication. The MA results for the 2 mm thickness sample, illustrated in graph 2, indicate a notably poor outcome with negative values. On the other hand, the 3 mm thickness sample demonstrates positive results, closely approaching 5-8% MA across the entire 2-8 GHz frequency range. Sample with thicknesses of 4 mm and 5 mm exhibit more satisfactory outcomes, with MA percentages ranging from approximately 20-60% and 40-75% for the 2-8 GHz frequency range, respectively.

F. Dielectric constant

The dielectric constant is defined as the ratio of the material's permittivity (Ɛ') to the permittivity of vacuum. Permittivity is measured in Farads per meter (F/m or $F.m^{-1}$), and the permittivity of vacuum, also known as the dielectric constant, is represented as 8.85×10-12 F/m. Typically, permittivity is also referred to as the relative permittivity of materials, signifying the materials' capacity to gather and store energy in the form of electrical charge within the polarization of the medium.

$$K=Ɛr=Ɛ_m/ Ɛ_0$$

Where Dielectric constant (K) = Relative Permittivity (Ɛr) = Permittivity of Material ($Ɛ_m$)/ Permittivity of Vacuum ($Ɛ_0$). Synthesized sample was tested for dielectric property with help of dielectric probe which gives the result in the form of real part permittivity (Ɛ') and dielectric loss (Ɛ" / Ɛ'). The imaginary part permittivity calculated as shown below.

$$Ɛ'=(Ɛ" / Ɛ') \times Ɛ"$$

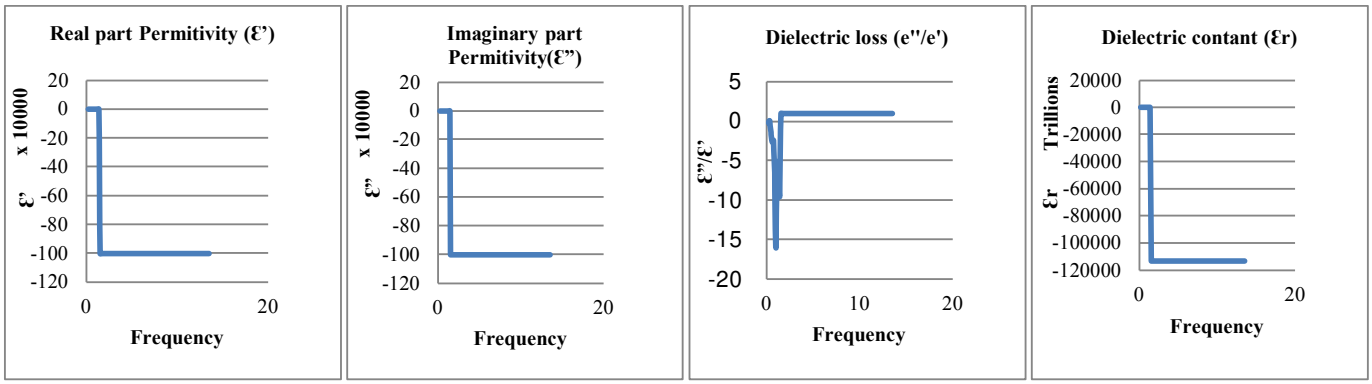

Fig.6. Real part Permittivity (e'), Imaginary part Permittivity (e"),Dielectric loss (e"/e'),Dielectric constant (Ɛr)

The real part of permittivity (Ɛ') signifies the stored electrical energy within a material, while the imaginary part of permittivity (Ɛ") indicates the loss of electrical energy. The dielectric loss factor (Ɛ" / Ɛ') serves as a measure of the material's power loss relative to the stored power. The dielectric constant of the synthesized material was assessed at ambient temperature across a frequency range from 10^8 to 10^10 Hz, as illustrated in Figure 6.

The real part of permittivity for the prepared sample exhibited positivity from 2.1×10^8 Hz to 1.41×10^9 Hz, transitioning to negative permittivity from 1.54 ×10^9 Hz to 1.35×10^10 Hz. The lowest observed permittivity value was -1000000 within the frequency range of 1.54 ×10^9 Hz to 1.35×10^10 Hz. The imaginary part of permittivity displayed similar values or trends to those observed in the real part of permittivity.

The dielectric loss of the obtained sample manifested negative values from 2.1×10^8 Hz to 1.41×10^9 Hz, and within the frequency range of 1.54 ×10^9 Hz to 1.35×10^10 Hz, a constant value of 1 was observed. The dielectric constant of the presented materials in this work demonstrated excellence, with the observed values, as shown in Figure 6, being -1000000×8.85×10^12.

IV. CONCLUSION

The CNMs were synthesized using a plant-based precursor (cotton) through the pyrolysis or carbonization method. Analysis through SEM and TEM confirmed that the resulting carbon materials exist in a nano form, featuring a diameter of 357.3 nm and tubular structures with thickness ranging from 30 to 50 nm. These carbon particles are adorned with metal nanoparticles, each having a size between 50-70 nm. Both Raman spectrograph and XRD affirmed the presence of crystalline and amorphous CNM, with copper nanoparticles (as per the Standard powder diffraction card of JCPDS, copper file No. 04-0836) uniformly distributed across the carbon surface. Despite exhibiting low microwave absorption performance, the prepared material showcases exceptional negative dielectric permittivity and dielectric constant values, positioning it as an outstanding candidate for superconducting materials.

REFERENCES

[1] T. D. Huan, S. Boggs, G. Teyssedre, C. Laurent, M.Cakmak, S. Kumar and R. Ramprasad, Prog. Mater.Sci., 2016, 83, 236-269.
[2] Z. Yao, Z. Song, H. Hao, Z. Yu, M. Cao, S. Zhang, M.T. Lanagan and H. Liu, Adv. Mater., 2017, 29, 1601727.
[3] L. Yang, X. Kong, F. Li, H. Hao, Z. Cheng, H. Liu, J.F.Li and S. Zhang, Prog. Mater. Sci., 2019, 102, 72-108.

[4] W. Hu, K. Lau, Y. Liu, R. L. Withers H. Chen, L. Fu, B.Gong and W. Hutchison, Chem. Mater., 2015, 27, 4934-4942.
[5] C. Zhao and J. Wu, ACS Appl. Mater. Interfaces, 2018,10, 3680-3688.
[6] Smith DR, Pendry JB, Wiltshire MC. Metamaterials and negative refractive index. Science.2004;305(5685):788-92.
[7] Fang N, Lee H, Sun C, Zhang X. Sub-diffraction-limited optical imaging with a silversuperlens. Science. 2005;308(5721):534-7.
[8] Liu Y, Zhang X. Metamaterials: a new frontier of science and technology. Chemical SocietyReviews. 2011;40(5):2494-507.
[9] Lu X, Shapiro MA, Mastovsky I, Temkin RJ, Conde M, Power JG, et al. Generation ofhigh-power, reversed-Cherenkov wakefield radiation in a metamaterial structure. PhysicalReview Letters. 2019;122(1):014801.
[10] N. Engheta , An idea for thin subwavelength cavity resonators using metamaterials with negative permittivity and permeability, IEEE Anten. Wirel. Propag. Lett. 1 (2002) 10–13.
[11] D. Schurig , J. Mock , B. Justice , S.A. Cummer , J.B. Pendry , A. Starr , D. Smith , Metamaterial electromagnetic cloak at microwave frequencies, Science 314 (5801) (2006) 977–980 .
[12] J. Wang , Z. Shi , F. Mao , S. Chen , X. Wang , Bilayer polymer metacomposites con- taining negative permittivity layer for new high-k materials, ACS Appl. Mater. Interfaces 9 (2) (2017) 1793–1800.
[13] Z. Shi , J. Wang , F. Mao , C. Yang , C. Zhang , R. Fan , Significantly improved di- electric performances of sandwich-structured polymer composites induced by alternating positive-k and negative-k layers, J Mater. Chem. A 5 (28) (2017) 14575–14582.
[14] M. Hoffmann , M. Peši ´c , K. Chatterjee , A.I. Khan , S. Salahuddin , S. Slesazeck , U. Schroeder , T. Mikolajick , Direct observation of negative capacitance in poly- crystalline ferroelectric HfO 2 , Adv. Funct. Mater. 26 (47) (2016) 8643–8649 .
[15] Y.-F. Hou , W.-L. Li , T.-D. Zhang , Y. Yu , R.-L. Han , W.-D. Fei , Negative capacitance in BaTiO 3 /BiFeO 3 bilayer capacitors, ACS Appl. Mater. Interfaces 8 (34) (2016) 22354–22360 .
[16] C. Liu , Y. Bai , L. Jing , Y. Yang , H. Chen , J. Zhou , Q. Zhao , L. Qiao , Equivalent en- ergy level hybridization approach for high-performance metamaterials design, Acta Mater. 135 (2017) 144–149 .
[17] Z. Wang , X. Fu , Z. Zhang , Y. Jiang , M. Waqar , P. Xie , K. Bi , Y. Liu , X. Yin , R. Fan , Paper based metasurface: turning waste-paper into a solution for electromag- netic pollution, J. Clean. Prod. 234 (10) (2019) 588–596.
[18] Lili Sun, Nan Wu Negative dielectric permittivity of PVDF nanocomposites induced by carbon nanofibers and polymer crystallization, Rui Peng, J Appl Polym Sci. 2020;e49582., https://doi.org/10.1002/app.49582
[19] Guohua Fan, Zhongyang Wang, Kai Sun, Yao Liu, Runhua Fa, Doping-dependent negative dielectric permittivity realizedin mono-phase antimony tin oxide ceramicsJ. Mater. Chem. C, 2020, DOI: 10.1039/D0TC02266G.
[20] Zhongyang Wang, Kai Sun,Peitao Xie, Qing Hou, Yao Liu, Qilin Gu, Runhua Fan, Design and analysis of negative permittivity behaviors in barium titanate/nickel metacomposites, Acta Materialia 185 (2020) 412–419, 359-6454/© 2019 Acta Materialia, https://doi.org/10.1016/j.actamat.2019.12.034
[21] Cheng C, Jiang Y, Sun, X. Shen, J Wang, T Fan, G Fan,Tunable negative permittivity behavior and electromagnetic shielding performance of silver/silicon nitride metacomposites,Composites: Part A (2019), doi: https://doi.org/10.1016/j.compositesa.2019.105753
[22] W. Chen, B. Qu, Chem. Mater., 2003, 15, 3208-3213, doi: 10.1021/cm030044h.
[23] W. Chen, L. Feng, B. Qu, Solid State Commun., 2004, 130, 259-263, doi: 10.1016/j.ssc.2004.01.031.
[24] H. Acharya, S. Srivastava, A. Bhowmick, Compos. Sci. Technol., 2007, 67, 2807-2816, doi: 10.1016/j.compscitech.2007.01.030.
[25] S. Srivastava, M. Pramanik, H. Acharya, J. Polym. Sci. Pol. Phys., 2006, 44, 471-480, doi: 10.1002/polb.20702.
[26] M. Maiti, A. Bhowmick, Compos. Sci. Technol., 2008, 68, 1-9, doi: 10.1016/j.compscitech.2007.05.042.
[27] P. Yang, H. Zhao, Y. Yang, P. Zhao, X. Zhao, L. Yang, ES Mater. Manuf., 2020, 7, 34-39, doi: 10.30919/esmm5f618.
[28] Haikun Wu, Haowei Sun, Fengjin Han, Peitao Xie, Yiming Zhong, Bin Quan, Yaman Zhao, Chunzhao Liu, Run hua Fan, Zhanhu Guo, Negative Permittivity Behavior in Flexible Carbon Nanofibers Polydimethylsiloxane Films Eng. Sci., 2022, 17, 113–120, DOI: https://dx.doi.org/10.30919/es8d576
[29] Bholanath Mukherjee, ShyambabuSainik, Vikaskumar Gupta, Kailash Jagdeo,Microwave absorption effiency of CNM decorated with cobalt nanoparticle, 2021 IJCRT | Volume 9, Issue 6 June 2021 | ISSN: 2320-2882.
[30] Maheshwar Sharon, Madhuri Sharon, GolapKalita and Bholanath Mukherjee, Hydrogen Storage by Carbon Fibers Synthesized by Pyrolysis of Cotton Fibers, Carbon Letters, Vol. 12, No. 1 March 2011 pp. 39-43. [CrossRef]
[31] Bholanath Mukherjee, Vikaskumar Gupta, Kailas Jagdeo, Madhuri Sharon, Hydrogen adsorption study of metal nanoparticle decorated carbon nanofiber, IJCRT | Volume 9, Issue 3 March 2021, 3646-3650
[32] Isaac Childres, Luis A. Jaureguib, WonjunParkb, Helin Cao, Yong P. Chen, Raman Spectroscopy of Graphene and related materials, Chapter 19.
[33] Mildred S. Dresselhaus, Ado Jorio, Mario Hofmann, Gene Dresselhaus, Riichiro Saito, Perspectives on Carbon Nanotubes and Graphene Raman Spectroscopy, Nano Lett., 10 (3), pp 751–758, 2010, DOI: 10.1021/nl904286r
[34] N Hikmah, N F Idrus, J Jai, A Hadi, Synthesis and characterization of silver-copper core-shell nanoparticles using polyol method for antimicrobial agent, Earth and Environmental Science 36 (2016). doi:10.1088/1755-1315/36/1/012050.
[35] T. Theivasanthi, M. Alagar , X-Ray Diffraction Studies of Copper Nanopowder, Archives of Physics Research, 2010, 1 (2):112-117, Scholars research library, ISSN 0976-0970.
https://doi.org/10.48550/arXiv.1003.6068
[36] Bholanath T.Mukherjee, Shyambabu. K.Sainik, Taguchi Optimization Methodology Directed Synthesis of CNMs from Plant Fibres Decorated with Metal Nano Particles for Study of Microwave Absorption in S and C Bands,IJRTE, ISSN: 2277-3878 (Online), Volume-11 Issue-3, September 2022, 10.35940/ijrte.C7263.0911322.
[37] Bholanath T. Mukherjee, Shyambabu. K. Sainik, Study of Reflection Loss In Ku Band By CNM Decorated With Metal Nano Particles, IJRASET,ISSN: 2321-9653,Volume 10 Issue IX Sep 2022,https://doi.org/10.22214/ijraset.2022.46644.
[38] B. T. Mukherjee,S. K. Sainik, K. R. Jagdeo, Microwave absorption by CNM decorated with nickel nano particles, IJESI, ISSN(online)2319–6734,ISSN(Print):2319–6726,Volume-6, Issue 9,September 2017, P P.77-80.
[39] Suyash S. Prasad, Shyambabu K. Sainik, Manoj D. Basutkar, Bholanath T. Mukherjee, Bimetal Decorated Carbon Nano Materials (CNMs) Synthesized from Plant Waste Materials as An Excellent Hydrogen Storage Material, IJRASET, ISSN: 2321-9653,Volume 10 Issue X Oct 2022.

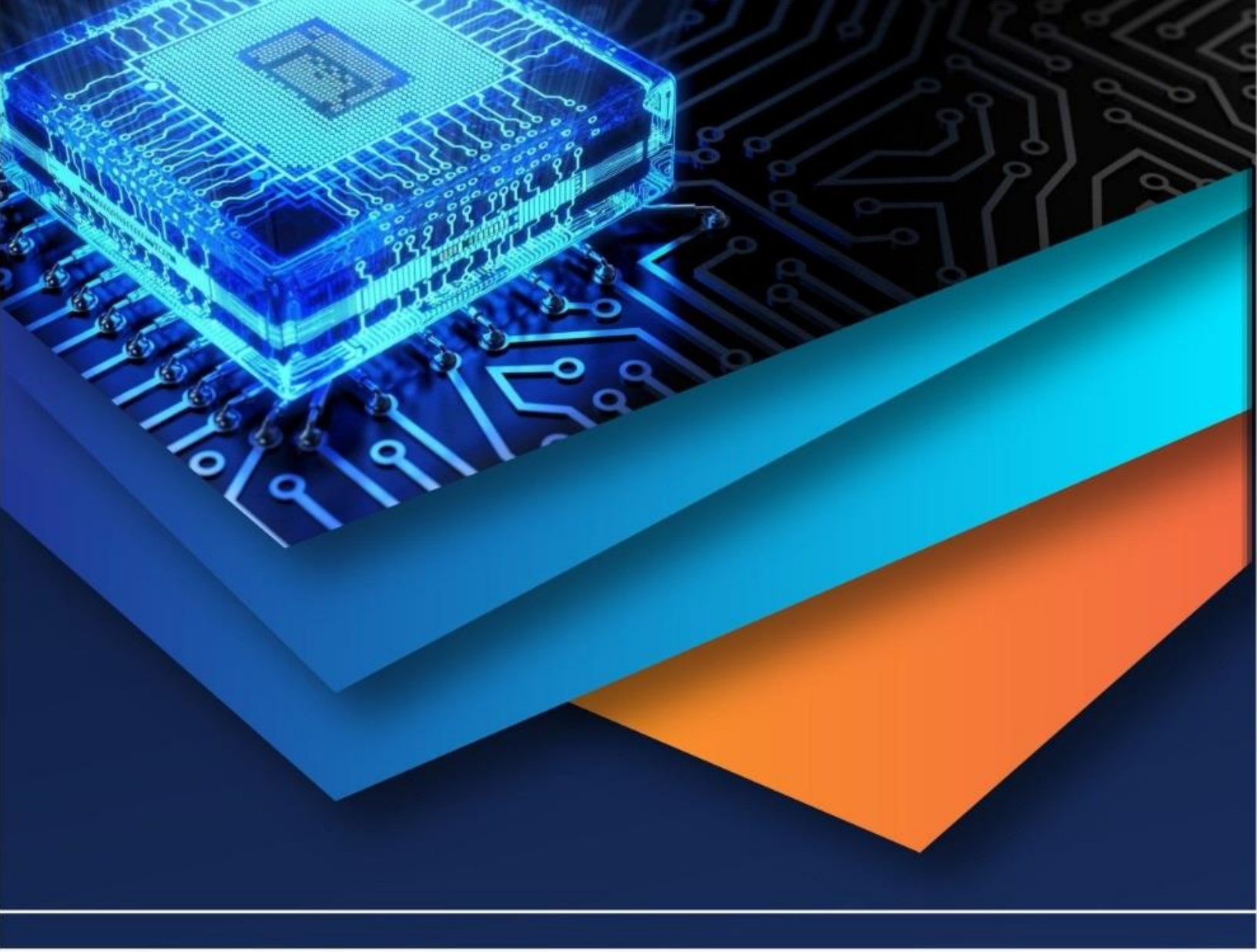

10.22214/IJRASET

45.98

IMPACT FACTOR: 7.129

IMPACT FACTOR: 7.429

INTERNATIONAL JOURNAL FOR RESEARCH

IN APPLIED SCIENCE & ENGINEERING TECHNOLOGY